



Check for updates

RESEARCH ARTICLE OPEN ACCESS

Feasibility of Deuterium Metabolic Magnetic Resonance Spectroscopy for the Investigation of Ischemia and Reperfusion in Rat Brain Slices Perfused Ex Vivo

Sarah Abendanan^{1,2} | David Shaul^{1,2} | J. Moshe Gomori¹ | Rachel Katz-Brull^{1,2}

¹Department of Radiology, Hadassah Medical Organization and Faculty of Medicine, Hebrew University of Jerusalem, Jerusalem, Israel | ²The Wohl Institute for Translational Medicine, Hadassah Medical Organization, Jerusalem, Israel

Correspondence: Rachel Katz-Brull (rachel.katz-brull@mail.huji.ac.il)

Received: 27 November 2024 | Revised: 23 July 2025 | Accepted: 25 July 2025

Funding: This work was supported by European Commission (101185775), Israel Innovation Authority (84405), and the Israel Ministry of Science, Innovation and Technology (1001704106/0006244).

ABSTRACT

Investigating glucose metabolism in the brain using $[6,6^{-2}H_2]$ glucose $(^2H_2$ -Glc) and deuterium-based NMR spectroscopy has shown promise for noninvasive monitoring of the fate of this labeled compound. This approach has already been applied in vivo in small animals and human subjects. A model of perfused rat brain slices recently showed promise for the investigation of the metabolic consequences of acute ischemic stroke, which is a significant cause of death and morbidity worldwide. The current study aimed to implement the deuterium-based glucose metabolism monitoring approach to study the metabolic consequences of ischemia and reperfusion in the rat brain ex vivo. In agreement with previous studies, we found that deuterated lactate $(^2H_2$ -Lac) was immediately formed in the brain upon administration of 2H_2 -Glc to the perfusion medium. This metabolite remained the predominant metabolic fate observed in the 2H -NMR spectra. Upon perfusion arrest, 2H_2 -Lac quickly built up to the same amount of 2H_2 -Glc eliminated from the medium engulfing the slices, reaching fivefold to sixfold its baseline level (n=6, three animals, and two ischemic conditions in each). Upon reperfusion, 2H_2 -Lac decreased to its level before the ischemic condition, and 2H_2 -Glc returned to its baseline. 2H_2 -Lac washout to the medium amounted to 2.2% of the 2H_2 -Lac signal associated with the slices after about 5 h of perfusion with 2H_2 -Glc, suggesting that the 2H_2 -Lac signal observed during the experiments was predominantly intracellular. These results demonstrate the utility of 2H_2 -Glc and 2H -NMR in monitoring the consequences of ischemia and reperfusion in the perfused rat brain slices model.

1 | Introduction

Acute ischemic stroke (AIS) is a significant cause of death and morbidity worldwide [1]. Ischemic brain tissue during a stroke is tissue at risk, which may be salvageable upon reperfusion. In addition to the temporary arrest of flow and the supply of oxygen and glucose (Glc), damage to the ischemic brain is also associated with reperfusion. Metabolically, the brain is the most energy-consuming organ and has a critical dependence on blood flow for its immediate supply of oxygen and Glc [2]. Interruption

of flow and supply of oxygen or Glc due to compromised pulmonary or cardiovascular function results in encephalopathy and, ultimately, cell death. Although Glc is the primary energy substrate for the brain, alternative substrates, such as lactate and ketone bodies, may be used under certain circumstances, such as starvation [3, 4]. Therefore, an investigation into the metabolic consequences of ischemia is warranted.

Nuclear magnetic resonance (NMR) spectroscopy or magnetic resonance spectroscopic imaging (MRSI) are noninvasive

This is an open access article under the terms of the Creative Commons Attribution-NonCommercial-NoDerivs License, which permits use and distribution in any medium, provided the original work is properly cited, the use is non-commercial and no modifications or adaptations are made.

© 2025 The Author(s). NMR in Biomedicine published by John Wiley & Sons Ltd.

biochemical analysis techniques that provide high-resolution spectra or images, respectively, of biological samples (ex vivo) or internal tissues (in vivo, noninvasively). For this reason, NMR and MRSI have been used in numerous studies of the metabolic aspects of cerebral ischemia. ³¹P-NMR of the highenergy phosphates and inorganic phosphate in the brain allows monitoring of the tissue's ATP content and pH value, respectively. In this way, ³¹P-NMR spectroscopy has been previously utilized for studies of AIS, both ex vivo [5, 6] and in vivo in animals [7] and in human subjects [8]. Hyperpolarized ¹³C-NMR of [1-13C]pyruvate metabolism, which allows monitoring of the metabolic fluxes of lactate dehydrogenase (LDH) and pyruvate dehydrogenase (PDH), was previously used for the investigation of these metabolic fluxes under ischemia and reperfusion conditions in perfused rat brain slices and showed an increase in LDH activity and a decrease in PDH activity during ischemia [9, 10]. Therefore, NMR spectroscopic methods have been useful so far in studying the overall highenergy condition and pH of the ischemic brain (31P-NMR) and the short-term metabolic fate of hyperpolarized substrates (hyperpolarized ¹³C-NMR). However, changes to metabolic fluxes on a time scale that is relevant to the clinical condition of stroke, that is, tens of minutes to hours, have not been characterized so far.

Deuterium metabolic imaging (DMI) is a novel, noninvasive MRSI approach that combines deuterium magnetic resonance spectroscopic imaging with oral intake or intravenous infusion of non-radioactive deuterium-labeled Glc to generate three-dimensional metabolic maps of the brain [11, 12]. DMI with the administration of [6,6- $^2\mathrm{H}_2$]Glc, ($^2\mathrm{H}_2$ -Glc) shows signals in the brain that are due to $^2\mathrm{H}_2$ -Glc, [3,3- $^2\mathrm{H}_2$]lactate ($^2\mathrm{H}_2$ -Lac), and deuterium-labeled-glutamate and -glutamine ($^2\mathrm{H}_x$ -Glx) [11, 12]. Figure 1 shows the flow of labels from $^2\mathrm{H}_2$ -Glc to $^2\mathrm{H}_2$ -Lac. $^2\mathrm{H}_x$ -Glx production results from incorporating [3,3- $^2\mathrm{H}_2$]pyruvate (Figure 1) into the citric acid cycle.

Pharmaceutical interventions for the treatment of stroke are scarce. Preclinical models of ischemic stroke are a limiting factor in the development of new therapies, as in vivo models of stroke in rodents suffer from a small and heterogeneous ischemic penumbra, and studies in large animals bear surgical complications and high costs [13]. These properties limit research into the metabolic consequences of this fragile tissue state and the development of corresponding therapeutics for this condition.

Here, we have used a perfused rat brain slice model, which may provide an alternative, ex vivo model for ischemic stroke research. This model enables the generation of a homogeneous ischemic brain tissue and monitoring of the metabolic response to an ischemic insult and reperfusion. In this model, environmental conditions can be regulated and monitored. For example, as previously described, perfusion can be controlled (to simulate stroke and reperfusion) [9, 10].

The current study aimed to investigate the metabolism of 2H_2 -Glc in the perfused rat brain slice model and characterize this tissue metabolism in the non-perturbed brain slices and brain slices under conditions of ischemia and reperfusion. We hypothesized that under ischemia, 2H_2 -Lac would increase (reflecting

oxygen deprivation stress) and that following reperfusion, this level should decrease (reflecting recovery). This study was driven by the hope that these metabolic flux characteristics, if indeed validated, could potentially serve as markers of salvageable brain tissue under stroke.

2 | Materials and Methods

2.1 | Chemicals

 $[6,6^{-2}\mathrm{H}_2]\mathrm{D}$ -glucose was obtained from Cambridge Isotope Laboratories (Tewksbury, MA, USA). NaCl, KCl, D-glucose, NaHCO $_3$, MgSO $_4$, NaH $_2$ PO $_4$, N-methyl-D-glucamine (NMDG), HEPES, pyruvic acid, ascorbic acid, thiourea, and CaCl $_2$ were purchased from Sigma-Aldrich (Rehovot, Israel). Isoflurane was obtained from the Institutional Authority for Biological and Biomedical Models of the Hebrew University (Jerusalem, Israel).

2.2 | Animals

Male Sprague–Dawley rats (n=4, 70–100g) were obtained from the Hebrew University Authority of Biological and Biomedical Models. The joint ethics committee (IACUC) of the Hebrew University and Hadassah Medical Center approved the study protocol for animal welfare. The Hebrew University is an AAALAC internationally accredited institute. Care was taken to minimize the animals' pain and discomfort. Animals were housed in the animal facilities 3–5 days after delivery for acclimatization and fed *ad libitum*. On the experimental day, animals were transferred to the laboratory and anesthetized within 1 h of arrival.

2.3 | Surgery and Brain Slices

Brain slices were extracted and maintained using the solutions described below, as previously described [9, 10]. Briefly, the rats were anesthetized using a gas anesthesia system (Somnosuite, Kent Scientific, Torrington, CT, USA). Induction was performed in a chamber with 3.5% isoflurane in room air with a flow rate of 440 mL/min. Following 4-7 min of induction, anesthesia was maintained with 3.1%-3.2% isoflurane at the same flow rate. Upon obtaining a negative pedal pain reflex, surgery was initiated. First, the diaphragm was exposed and cut, and the rat was transcardially perfused with 30 mL of ice-cold NMDG-aCSF (Solution 1, below). The animals were then sacrificed by decapitation, and the brain was rapidly removed and placed in icecold NMDG-aCSF (Solution 1, below). The cerebrum was then cut into four parts (first, a sagittal cut along the hemispheric cleft and then a sagittal cut in the middle of each hemisphere). From each part, 350-µm slices were prepared using a McIlwain tissue chopper (The Mickle Laboratory Engineering Company Ltd., Surrey, UK). The process of brain extraction, from decapitation until the brain was in ice-cold NMDG-aCSF, took under 2 min, and the slicing procedure was done in less than 10 min. After cutting, the slices were transferred to warm, 32°C-34°C, NMDG-aCSF (Solution 1, below) for 12 min for protective recovery. Then, the slices were transferred to HEPES-holding aCSF (Solution 2, below) at ~32°C for 15-40 min incubation before

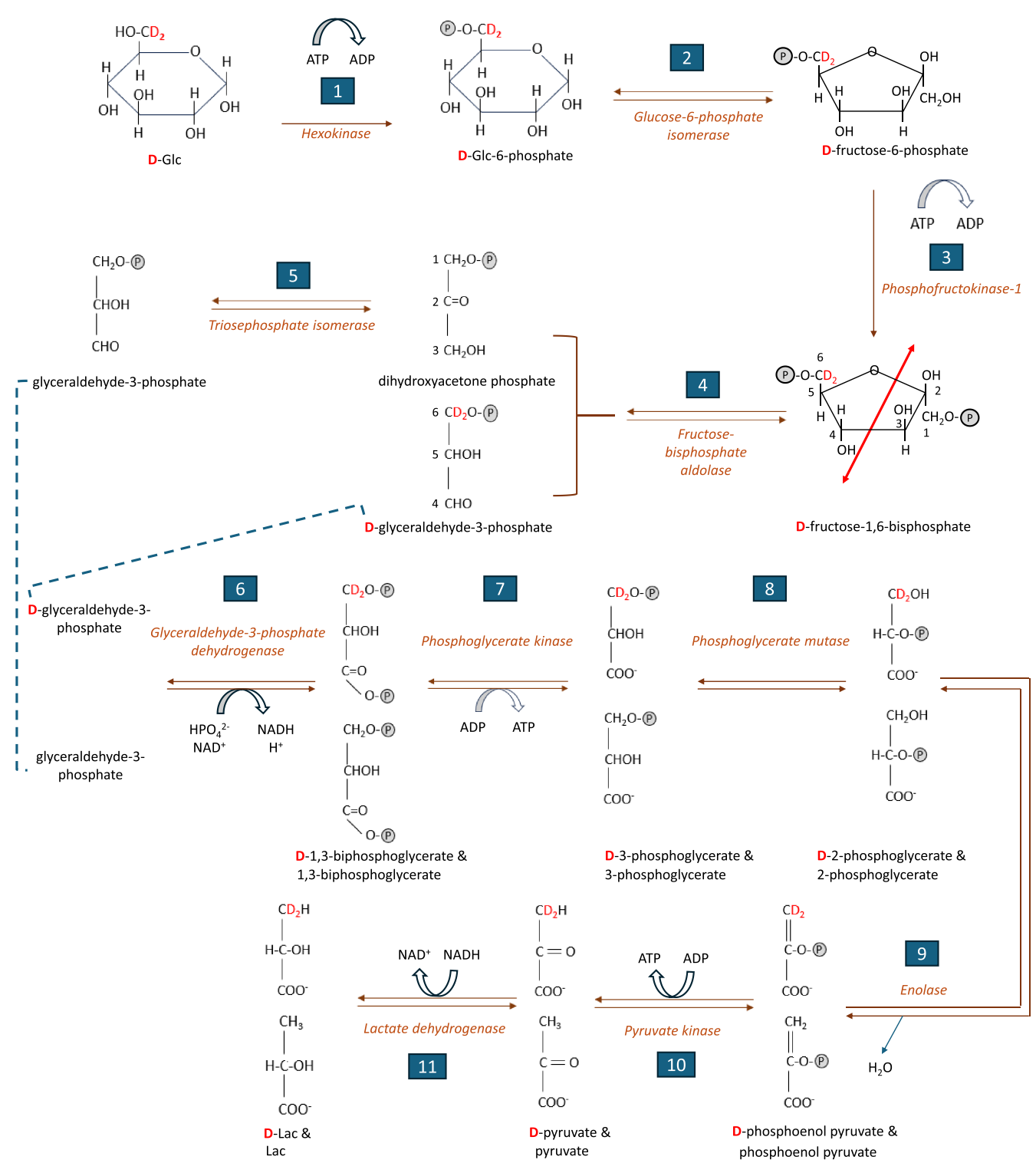


FIGURE 1 | The glycolysis pathway, followed by the lactate dehydrogenase reaction, shows the fate of the two-deuteron label of ${}^2\mathrm{H}_2$ -Glc. This scheme provides the basis for quantifying the deuterated-lactate signal relative to the signals of the natural abundance of deuterium in water and the deuterated glucose in the ${}^2\mathrm{H}$ NMR spectra. **D** (red) in the compound's name marks the label with two deuterons (${}^2\mathrm{H}_2$, in a single molecule, not to be confused with dextrorotatory). This scheme illustrates that each ${}^2\mathrm{H}_2$ -Glc (**D**-Glc) molecule yields one ${}^2\mathrm{H}_2$ -Lac (**D**-Lac) molecule and one unlabeled lactate molecule. The red arrow on ${}^2\mathrm{H}_2$ -fructose-6-phosphate (**D**-fructose-6-phosphate) marks the cleavage sites of phosphofructokinase. Encircled "P" marks a PO₃ moiety. Abbreviations: Glc, glucose; Lac, lactate; **D**-Glc, [6,6- ${}^2\mathrm{H}_2$]D-glucose; **D**-Glc-6-phosphate, [6,6- ${}^2\mathrm{H}_2$]D-glucose-6-phosphate; **D**-fructose-6-phosphate, [6,6- ${}^2\mathrm{H}_2$]fructose-1,6-bisphosphate; **D**-glyceraldehyde-3-phosphate, [3,3- ${}^2\mathrm{H}_2$]glyceraldehyde-3-phosphate; **D**-fructose-1,6-bisphosphate; **D**-glyceraldehyde-3-phosphate; **D**-glyceraldehyde-3-phosphosphate; **D**-1,3-biphosphoglycerate, [3,3- ${}^2\mathrm{H}_2$]1,3-biphosphoglycerate; **D**-3-phosphoglycerate, [3,3- ${}^2\mathrm{H}_2$]3-phosphoglycerate; **D**-phosphoglycerate; **D**-phosphoglycerate; **D**-phosphoglycerate; **D**-pyruvate, [3,3- ${}^2\mathrm{H}_2$]pyruvate; **D**-Lac, [3,3- ${}^2\mathrm{H}_2$]1-phosphoglycerate; **D**-phosphoglycerate; **D**-pyruvate, [3,3- ${}^2\mathrm{H}_2$]pyruvate; **D**-Lac, [3,3- ${}^2\mathrm{H}_2$]1-glactate.

transfer to the NMR spectrometer, where the slices were perfused with the Perfusion aCSF (Solution 3, below).

2.4 | Solutions

To improve the health of acute brain slices obtained from mature adult rats, we modified a slice preparation technique optimized for in vitro electrophysiology in mature adult rat brain slices [14]. In brief, slice health is improved by a so-called "protective recovery" method. NMDG is an extracellular replacer of sodium ions that prevents sodium ions and water influx into cells, the primary insult causing cell death following brain slicing. Ting et al. showed that the presence of NMDG during a 12-min recovery phase after slicing dramatically improved the health of acute slices from mature adult rats in electrophysiological recordings [14]. Furthermore, incubation in HEPES-buffered artificial cerebrospinal fluid (aCSF) improved slice health [14]. The following solutions were prepared in the current study, and their use is described in the following sections.

2.4.1 | Solution 1—NMDG-aCSF

NMDG-aCSF was used for transcardial perfusion, tissue slicing, and slice recovery. This medium contained 93-mM NMDG, 2.5-mM KCl, 1.2-mM $\rm NaH_2PO_4$, 26-mM $\rm NaHCO_3$, 20-mM HEPES, 25-mM D-glucose, 10-mM $\rm MgSO_4$, 0.5-mM $\rm CaCl_2$, 5-mM ascorbic acid, 2-mM thiourea, and 3-mM pyruvic acid in double-distilled water.

2.4.2 | Solution 2—HEPES-Holding aCSF

HEPES-holding aCSF was used to incubate slices following the surgical procedure. This medium contained 84-mM NaCl, 2.5-mM KCl, 1.2-mM NaH $_2$ PO $_4$, 30-mM NaHCO $_3$, 20-mM HEPES, 25-mM Glc (D-glucose, non-labeled), 2-mM MgSO $_4$, 2-mM CaCl $_2$, 5-mM ascorbic acid, 2-mM thiourea, and 3-mM pyruvic acid in double-distilled water.

2.4.3 | Solution 3—Perfusion aCSF

Perfusion aCSF was used for perfusion in the NMR spectrometer. This medium contained 115-mM NaCl, 2.5-mM KCl, 1.2-mM NaH $_2$ PO $_4$, 24-mM NaHCO $_3$, 5-mM HEPES, 10-mM Glc (to be replaced with 10-mM $^2\mathrm{H}_2$ -Glc), 2-mM MgSO $_4$, and 2-mM CaCl $_2$ in double-distilled water.

All three solutions (1–3) were bubbled with 95%/5% $\rm O_2/CO_2$ for at least 1 h before use and titrated to a pH of 7.35–7.45 using HCl or NaOH. All concentrations were optimized for a calculated osmolarity of 310 \pm 15 mOsm.

2.5 | Oxygen Concentration in the aCSF Solutions

The air pressure in our laboratory (located in Ein-Kerem, Jerusalem, Israel) is about 0.9 atm (900 m above sea level) or 684 mmHg. The partial oxygen pressure in the air, in the NMR

tube above the perfused slices, is therefore 143 mmHg. The aCSF solutions engulfing the slices were saturated with oxygen; therefore, the partial pressure of oxygen in them was 143 mmHg as well.

In vivo, the brain tissue oxygen concentration or partial pressure is typically within a range of 25–50 mmHg, which is lower than the partial oxygen pressure in the aCSF solutions. The reason for this difference and for the choice to work with oxygen-saturated media is that in perfused brain slices, in the absence of transport by the vasculature, oxygen arrives at the brain cells by diffusion from the slice surface to its inner core, with a maximal diffusion distance that is half of the slice thickness (350 μm), that is, 175 μm . The high partial oxygen pressure in the aCSF solutions provides an oxygen concentration gradient that leads to oxygen flux into the innermost parts of the slices. For this reason, the current study, as well as other studies of brain slices and other perfused tissue slices, is typically carried out using media saturated with oxygen.

2.6 | NMR Acquisitions

³¹P- and ²H-NMR spectroscopy were performed using a 5.8-T high-resolution NMR spectrometer (RS2D, Mundolsheim, France) with a 10-mm broadband NMR probe. The magnetic field lock system was applied during ³¹P-NMR acquisitions but not during ²H-NMR acquisitions.

³¹P-NMR FIDs were acquired with 782 or 1564 averages, a repetition time of 1.15s (temporal resolution of 15 or 30 min, respectively), a 50° flip angle, and 8192 time points.

²H-NMR FIDs were acquired with 80 averages, a repetition time of 1.5s (2min temporal resolution), a 90° flip angle, and 1024 time points. The deuterium lock system was used for this acquisition, using a modification to the channel routing system in the spectrometer made specifically for this type of acquisition by the manufacturer (RS2D, Mundolsheim, France).

An inversion-recovery acquisition carried out in physiological saline at 20°C, in the same spectrometer and NMR tube, showed that the $\rm T_1$ of $\rm ^2H_2\text{-}Glc$ deuterons was 53 ms and the $\rm T_1$ of H²HO was 420 ms. Therefore, the ²H-NMR data acquired here were acquired under near fully relaxed conditions and do not necessitate any adjustments for quantification related to $\rm T_1$ differences.

2.7 | Calculation of Deuterated Compounds' Concentrations From Deuterium NMR Spectra

The natural abundance of deuterium in water (the signal of H²HO) was used as an internal reference to calculate the concentration of the deuterated metabolites in the sample in each spectrum [15]. To reduce the variability of the data that may result from variations in this internal standard's signal and to allow changes in H²HO signal intensity to be manifested in the concentration analysis, the H²HO signal was first averaged over 10 spectra. Then, each H²HO signal in all the spectra was converted to concentration units in the following way:

$$[H^2HO] = S_{H2HO}^*17.16 / S_{AV_H2HO}$$

where $S_{\rm H2HO}$ is the individual H²HO signal in each spectrum, [H²HO] is the concentration equivalent of each $S_{\rm H2HO}$, and $S_{\rm AV_H2HO}$ is the averaged H²HO signal from the 10 spectra at the beginning of the experiment (during perfusion with 2H_2 -Glc). As the natural abundance of deuterium is 0.0156% and the concentration of protons in water is 110 M, the theoretical concentration of H²HO is 17.16 mM (0.0156%*110 M).

For $^2\mathrm{H}_2$ -Glc and $^2\mathrm{H}_2$ -Lac, there are two deuterium nuclei per molecule. Therefore, their concentrations ([$^2\mathrm{H}_2$ -Glc] and [$^2\mathrm{H}_2$ -Lac], respectively) were calculated as follows:

$$\left[^{2}\rm{H}_{2}-Glc\right]={\rm{S}_{2H2-Glc}}^{*}\left(17.16/\rm{S}_{\rm{AV}_{H2HO}}\right)/2$$

where $S_{2H2\text{-}Glc}$ is the individual signal of $^2H_2\text{-}Glc$.

and

$$[^{2}H_{2} - Lac] = S_{2H2-Lac}^{*}(17.16/S_{AV H2HO})/2$$

where $\rm S_{2H2\text{-}Lac}$ is the individual signal of $^2H_2\text{-}Lac.$

Note that the total concentration of lactate (deuterium-labeled lactate and non-labeled lactate combined) produced from $^2\mathrm{H}_2$ -Glc is twice that of $^2\mathrm{H}_2$ -Lac (Figure 1).

We note that the scheme in Figure 1 considers only the glycolysis pathway and does not include the possible shunting of the deuterium-labeled glucose-6-phosphate to the pentose phosphate pathway, which may result in the loss of some of the deuterium-labeled lactate and an increase in the H²HO signal. The latter was observed by Ben Yosef et al. in 1994 [16], in cultured rat 9L glioma cells. However, because we did not detect any significant increase in the H²HO signal in our experiments, we could not justify the inclusion of this consideration in the calculation of concentrations in the current study. Shunting glucose-6-phosphate to glycolysis or the pentose phosphate pathway is cell- and condition-dependent, as are all metabolic fluxes. It appears that in the current rat brain slice preparation, the effects of the shunting to the pentose phosphate pathway were not significant. We also note that this scheme does not support the possible production of a lactate molecule that is labeled with only one deuteron, which was suggested by de Graaf et al. in 2021 [17].

2.8 | Perfusion of Brain Slices in the NMR Spectrometer

The perfusion system was operated as described previously at $4\,\text{mL/min}$ [9, 18]. $^2\text{H}_2\text{-Glc}$ was introduced to the slices by adding it to the external aCSF reservoir. To allow the utilization of a minimal amount of the labeled compound, $70\,\text{mL}$ of aCSF was used for the perfusion of the slices with $^2\text{H}_2\text{-Glc}$.

2.9 | Spectral Analysis

Spectral processing and intensity integrals were calculated using MNova (Mestrelab Research, Santiago de Compostela, Spain).

2.10 | Statistical Analysis

Statistical analysis was performed in Excel (Microsoft Office, Rānana, Israel).

3 | Results

A typical time course of $^2\mathrm{H}_2$ -Glc metabolism in the perfused and ischemic brain is shown in Figure 2. Individual and averaged $^2\mathrm{H}_2$ -Glc and $^2\mathrm{H}_2$ -Lac levels in each experiment and within the various experimental sections are provided in Table S1 and Figure 3. Upon administration of $^2\mathrm{H}_2$ -Glc to the external reservoir of the perfusion medium, its signal (in the NMR tube) reached a plateau within $6 \, \mathrm{min} \, (8.6 \pm 0.7 \, \mathrm{mM})$. The $^2\mathrm{H}_2$ -Lac signal was observed within $8 \, \mathrm{min} \, \mathrm{of} \, \mathrm{the} \, ^2\mathrm{H}_2$ -Glc administration; it increased and reached a plateau of $0.9 \pm 0.4 \, \mathrm{mM} \, (n=3)$ within 12– $14 \, \mathrm{min}$.

The perfusion was arrested for $10\,\mathrm{min}$ (first ischemic condition) at $49-76\,\mathrm{min}$ (n=3) from the administration of $^2\mathrm{H}_2$ -Glc. During this period, the signal of $^2\mathrm{H}_2$ -Lac increased gradually to a maximal level of $5.1\pm1.3\,\mathrm{mM}$ (n=3), and the signal of $^2\mathrm{H}_2$ -Glc decreased gradually to a minimal level of $4.6\pm1.5\,\mathrm{mM}$ (n=3, two-tailed, paired t-test, before and at the end of the first ischemic condition, p=0.035). After the first ischemic condition, the perfusion was resumed. Upon reperfusion, within about $8\,\mathrm{min}$, the signal of $^2\mathrm{H}_2$ -Glc returned to the baseline level of $8.7\pm0.7\,\mathrm{mM}$ (n=3), and the signal of $^2\mathrm{H}_2$ -Lac returned to baseline at a level of $1.1\pm0.3\,\mathrm{mM}$ (two-tailed, paired t-test before and after ischemia, p=0.17, no difference). Continuous perfusion followed the first ischemic condition for $53-70\,\mathrm{min}$, and then the perfusion was again arrested for $10\,\mathrm{min}$ (second ischemic condition).

During the second ischemic condition, the ²H₂-Lac concentration gradually increased to a similar maximal level of $5.91 \pm 0.12 \,\mathrm{mM}$ (n = 3, two-tailed, paired t-test, first and second ischemic conditions, p = 0.50, no difference). The signal of ${}^{2}\mathrm{H}_{2}$ -Glc decreased to $4.1 \pm 0.5 \,\mathrm{mM}$, as in the first ischemic condition (n = 3, two-tailed, paired t-test, first and second ischemic conditions, p = 0.56, no difference, and two-tailed, paired t-test, before and at the second ischemic condition, p = 0.001). After the second ischemic condition, the perfusion was resumed, and again, within about 8 min, the ²H₂-Glc signal returned to the baseline level of $9.3 \pm 1.1 \,\mathrm{mM}$ (two-tailed, paired t-tests before the first ischemic condition and after the second ischemic condition, p = 0.2). The ${}^{2}\text{H}_{2}$ -Lac signal acquired after reperfusion (following the second ischemic condition) was similar to its level before the first ischemic condition and between the two ischemic conditions, indicating that ²H₂-Lac did not accumulate within the cells because of the ischemic conditions (p = 0.4, ANOVA with replication).

On both ischemic conditions, the increase in $^2\mathrm{H}_2$ -Lac concentration was the same as the maximal decrease in the $^2\mathrm{H}_2$ -Glc concentration (5.5 \pm 1.1 mM and 4.3 \pm 0.9 mM, respectively, n = 6, p = 0.2, no difference, two-factor ANOVA with replication). This suggested that the $^2\mathrm{H}_2$ -Glc available to the brain slices during the ischemic conditions was fully converted to $^2\mathrm{H}_2$ -Lac (and, by inference, also to the same amount of non-labeled lactate).

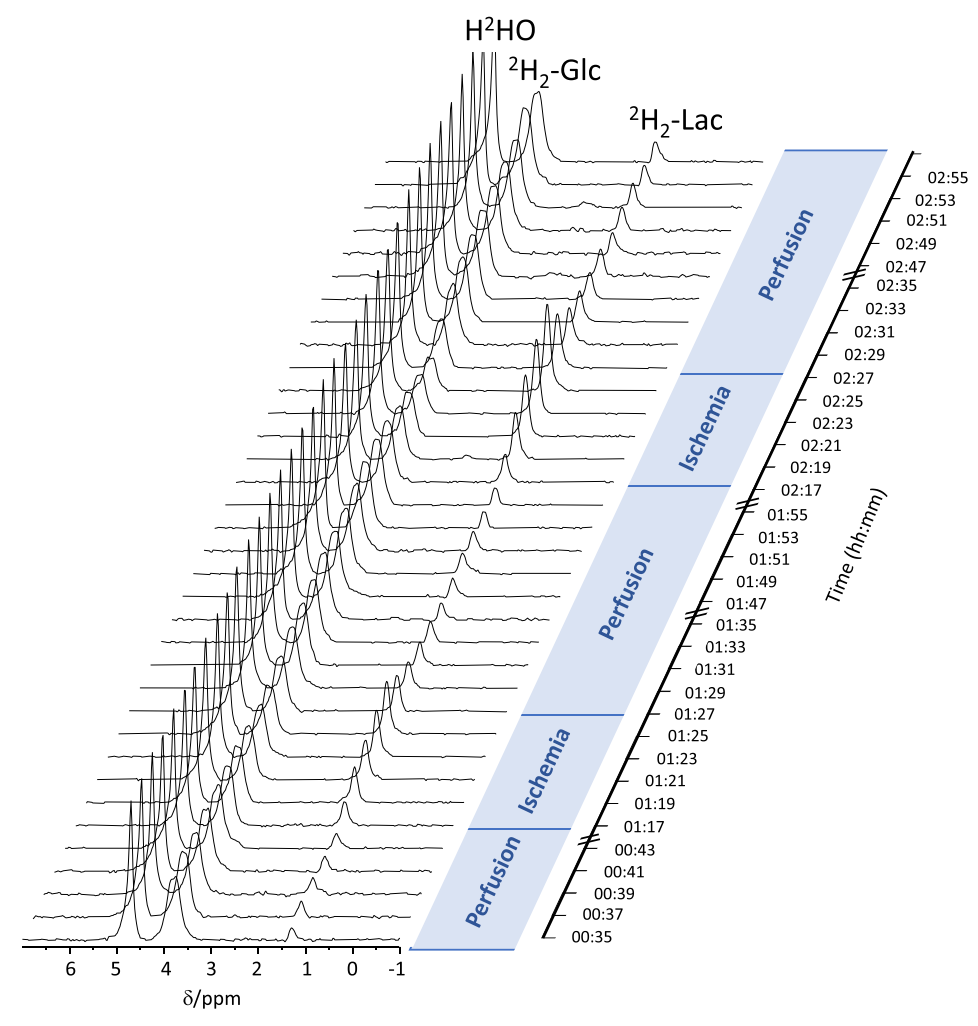


FIGURE 2 | Stacked deuterium NMR spectra of a typical experiment with two ischemic periods. The $\mathrm{H^2HO}$, $\mathrm{^2H_2}$ -Glc, and $\mathrm{^2H_2}$ -Lac signals are consistently observed and allow the calculation of the concentration changes during the ischemic conditions. The time scale is in hh:mm (h, hour; m, min). The addition of $\mathrm{^2H_2}$ -Glc to the external perfusion medium was taken as the starting time (00:00). The durations of continuous perfusion and flow arrest are marked as Perfusion and Ischemia, respectively. $\mathrm{H^2HO}$, the natural abundance of deuterium in water; $\mathrm{^2H_2}$ -Glc, [6,6- $\mathrm{^2H_2}$]D-glucose; $\mathrm{^2H_2}$ -Lac, [3,3- $\mathrm{^2H_2}$]lactate.

³¹P NMR spectra of the slices recorded before the first ischemic condition and after the second ischemic condition confirmed the viability of the slices and the consistent presence of ATP and PCr in the slices. The individual spectra are shown in Figure S1. Analysis of ATP content in the slices, comparing the state before the first ischemic condition and after the second ischemic condition, showed that during this time (about 5 h), it decreased by $28 \pm 5\%$ (n = 3, average \pm standard deviation). This analysis was based on the γ-ATP signal, as described previously [10].

In one of these experiments, we tested an additional third ischemic condition, which was applied at 87 min after the second ischemic condition for 64 min. In this third ischemic condition, the $^2\mathrm{H}_2\text{-Lac}$ concentration increased to 10.2 mM, and the $^2\mathrm{H}_2\text{-Glc}$ concentration decreased to 1.2 mM. A $^{31}\mathrm{P}$ spectrum acquired toward the end of this ischemic condition showed almost no highenergy phosphate signals (Figure S1G, Supporting Information). However, 30 min further to reperfusion, some recovery was observed (Figure S1H, Supporting Information). Interestingly, in this experiment, $^2\mathrm{H}_{\mathrm{v}}\text{-Glx}$ was sporadically observed during

the first ischemic condition and afterwards. The level of 2H_x -Glx increased toward the end of the long third ischemic condition (Figures 4 and S2).

In a control experiment without perfusion arrests (no ischemic conditions), the level of $^2\mathrm{H}_2\text{-Lac}$ was constant throughout, at a level similar to the three ischemia experiments under continuous flow. In a spectrum acquired without brain slices from the medium used for perfusion of these slices (without perfusion arrest) for 5 h, in the presence of $^2\mathrm{H}_2\text{-Glc}$ (acquired at the same perfusion flow), the $^2\mathrm{H}_2\text{-Lac}$ signal was found to be 2.2% of the level of $^2\mathrm{H}_2\text{-Lac}$ in the NMR tube containing the brain slices.

4 | Discussion

We have implemented here a metabolic flux approach that utilizes $^2\mathrm{H}_2$ -Glc as a metabolic substrate for perfused brain cells. The advantage of the isotopic label used here compared to other relevant magnetically active nuclei is briefly described below. Compared to proton spectroscopy, the deuterium label enables

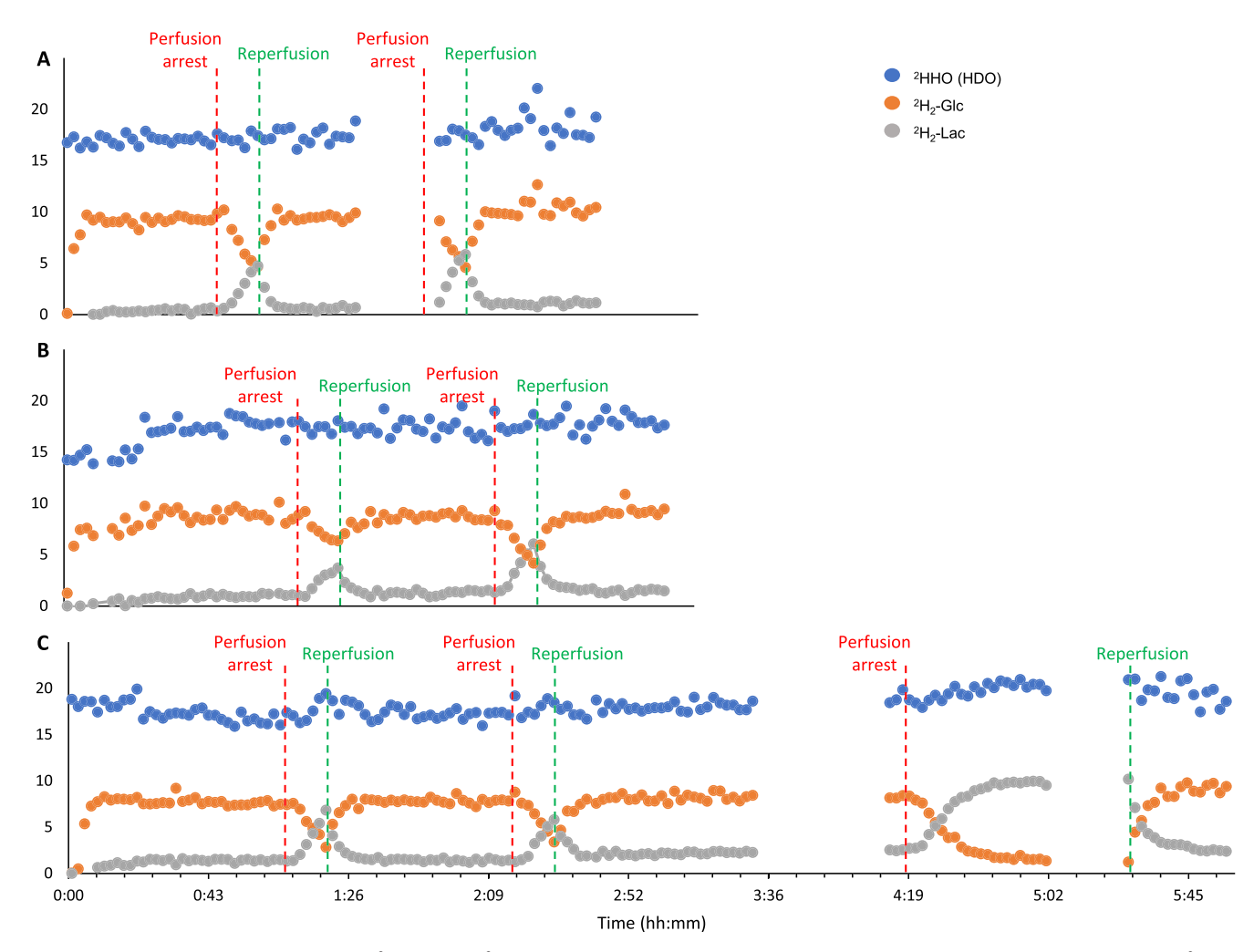


FIGURE 3 Individual time courses of ${}^{2}\text{H}_{2}$ -Glc and ${}^{2}\text{H}_{2}$ -Lac in brain slices on three experimental days (A, B, and C). The results show ${}^{2}\text{H}_{2}$ HO (HDO), ${}^{2}\text{H}_{2}$ -Glc, and ${}^{2}\text{H}_{2}$ -Lac concentrations in mM. The Y-axis is the concentration in the NMR tube in mM for the three species. Breaks in ${}^{2}\text{H}$ -NMR acquisitions were taken to record ${}^{31}\text{P}$ spectra.

the observation of newly formed metabolic pools and differentiates them from the steady-state levels of these metabolites. Proton spectroscopy (without isotopic labeling) will also show the steady-state levels of glucose and lactate, which are not expected to change without perturbation. In addition, for proton spectroscopy, water suppression should be applied, and this was not technically possible on our system. Compared to a ¹³C label, which has been utilized in numerous studies of Glc metabolism because of its wide chemical shift spectrum and ability to resolve metabolites, the deuterium label allows higher SNR per acquisition time due to the short T₁ of the deuterium label, despite the lower gyromagnetic ratio of deuterium compared to ¹³C. This allows studies with higher temporal resolution, even if at lower metabolite resolution. The same rationale led to the original DMI studies in the human brain [11, 12]. The use of the deuterium label also enables concentration calculation using the natural abundance of deuterium in water as a stable quantification reference, a property that is unique in NMR and is specifically useful in the current setup.

The results of this study show increased glucose-to-lactate conversion directly and in real time, in brain tissue during ischemia. The results also demonstrate that lactate is the predominant

product of glucose utilization under continuous flow and during ischemia. This result agrees with previous work by Hage et al. [19], who found that the main products of glucose metabolism in rat brain slices were lactate and ${\rm CO}_2$ (after 60 min of incubation). As ${\rm CO}_2$ does not carry a deuterium label, we could not detect it in the current study. However, ${}^2{\rm H}_2$ -Lac was identified as the primary metabolic fate.

Previously, using the same perfused brain slices model and with hyperpolarized [1^{-13} C]pyruvate and 13 C-NMR spectroscopy, we have shown that within 1 min of ischemia, [1^{-13} C]lactate production increased [9, 10]. Here, we have confirmed this observation over much longer durations of ischemia ($10 \, \text{min}$ and up to $64 \, \text{min}$), which could not be interrogated with hyperpolarized substrates because of the meta-stable nature of the hyperpolarized state. The observed increase in $^2\text{H}_2$ -Lac must be supported by a rise in $^2\text{H}_2$ -Glc uptake, as no other source of the deuterium label is available to the cells to produce $^2\text{H}_2$ -Lac. Under continuous perfusion, it is impossible to determine $^2\text{H}_2$ -Glc uptake in the current setup because the perfusion medium contains $^2\text{H}_2$ -Glc, which is continuously supplied into the NMR tube containing the brain slices (and then washes out). However, $^2\text{H}_2$ -Glc uptake during ischemia is directly demonstrated here as the

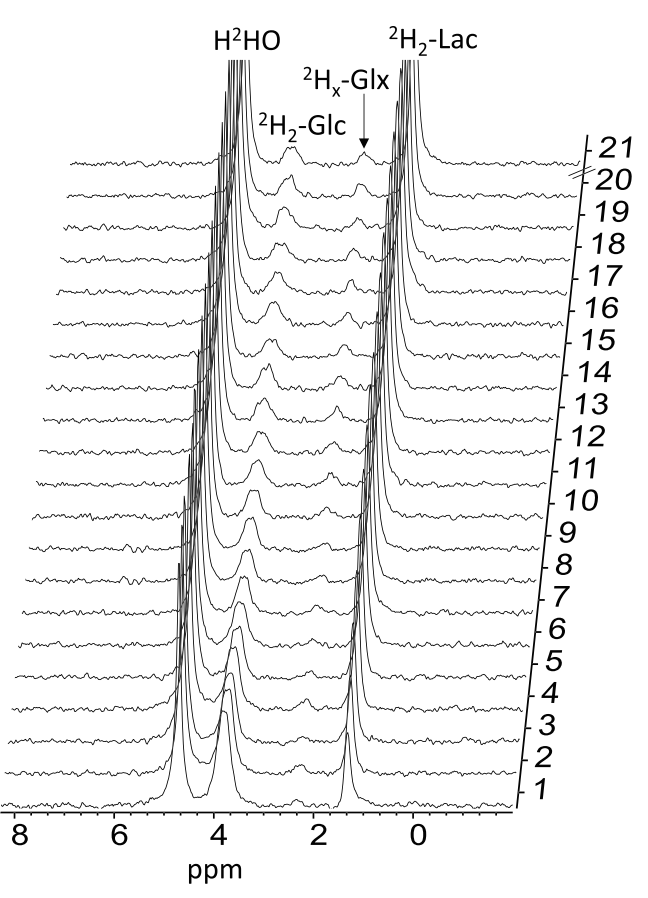


FIGURE 4 | Stacked deuterium NMR spectra of an experiment with three ischemic conditions. For clarity, only the third ischemic duration is shown. In addition to the $\rm H^2HO$, $^2\rm H_2$ -Glc, and $^2\rm H_2$ -Lac signals, which are consistently observed, the signal of $^2\rm H_x$ -Glx can also be observed. The data are shown at 2-min intervals starting at the beginning of the third ischemic condition and before reperfusion. The top spectrum, marked Spectrum 21, was acquired at the end of the third ischemic condition, 22 min after the spectrum marked 20, and after 62 min of ischemia. $\rm H^2HO$, the natural abundance of deuterium in water; $\rm ^2\rm H_2$ -Glc, $[6,6^2\rm H_2]\rm D$ -glucose; $\rm ^2\rm H_2$ -Lac, $[3,3^2\rm H_2]\rm lactate$; $\rm ^2\rm H_x$ -Glx, deuterium-labeled glutamine and glutamate.

depletion of ${}^2\mathrm{H}_2$ -Glc in the medium engulfing the brain slices during perfusion arrest.

In the literature, the effects of ischemia on cerebral Glc uptake are varied. In a model of middle cerebral artery occlusion in cats, Welsh et al. have observed a local increase in [14C]deoxyglucose uptake in some ischemic regions, interpreted as activation of Glc metabolism [20]. However, in the most severely ischemic areas with ATP depletion, the [14C]deoxyglucose level decreased, interpreted as limited Glc supply to these regions. Combs et al. induced global ischemia in gerbils and showed that elevated plasma Glc correlated with a linear increase in cerebral lactate [21].

In contrast to in vivo DMI studies, where $^2\mathrm{H}_2$ -Glc was administered systemically (preclinically and in humans, intravenously and *per os*, respectively), we did not observe a reproducible production of $^2\mathrm{H}_x$ -Glx, and its level appears lower than in the in vivo spectra compared to the $^2\mathrm{H}_2$ -Lac level. This observation

may indicate that the turnover, which results in the deuteration of Glx, is enhanced under severe stress conditions, as marked by the ATP depletion observed on ³¹P spectra (Figure S1G, Supporting Information), although this is an anecdotal observation. The notation ²H_x-Glx indicates that this signal originates from deuterated glutamine or glutamate, but that the number of deuterons per molecule is not known to us. This is because the Glx pool becomes labeled through turnover, not because of the net synthesis of Glx. We also note that the signal assigned to Glx may result from a different labeled metabolite altogether, possibly pyruvate. This aspect will be investigated in the future. The current study's lack of reproducible ²H_w-Glx signals may also suggest that ²H_v-Glx signals observed in vivo result from higher ²H_v-Glx turnover in other body organs rather than in situ in the brain. While glutamate uptake from the plasma to the brain is low, glutamine uptake from the blood into the brain is saturated at levels > 1 mM and may comprise a significant part of the brain's glutamine pool [22]. Deuterated glutamine that has been taken up into the brain can then be converted into deuterated glutamate. Observing consistent ²H_x-Glx signals in one of the experiments may suggest that it takes longer to observe in the brain than ²H₂-Lac. In this respect, in vivo DMI acquisitions typically occur 1-2h after ²H₂-Glc administration. However, it cannot be ruled out that this observation is related to the insult caused to the brain tissue by the extraction and the slicing procedures. Nevertheless, regardless of the cause, our results align with prior studies in perfused brain slices that showed lactate and CO₂ to be the main products of glucose metabolism [19].

Previously, we have shown the reversibility of tissue pH characteristics in the same perfused brain slice system as acidification during ischemia and return to neutral pH upon reperfusion, which is one of the hallmarks of the ischemic condition [9]. The reproducibility of the real-time $^2\mathrm{H}_2$ -Lac rise during ischemia and return to baseline upon reperfusion, as well as the $^2\mathrm{H}_2$ -Glc utilization characteristics in both ischemic episodes, further demonstrates that the current brain slice system is a valuable model for investigating the metabolic consequences of brain ischemia and reperfusion. Our findings may warrant utilizing this technology ($^2\mathrm{H-NMR}$ of $^2\mathrm{H}_2$ -Glc metabolism) and setup (perfused rat brain slices) to investigate the effects of neuroprotective agents. It may also suggest that $^2\mathrm{H-NMR}$ and DMI could be used to study the ischemic penumbra in vivo.

5 | Study Limitations

5.1 | Concentration Values

We note that the calculation of 2H_2 -Glc and 2H_2 -Lac concentrations refers to their concentrations in the NMR tube within the volume covered by the NMR probe. However, there are a few limitations to the concentration calculation (Materials and Methods): (1) Although the concentration of 2H_2 -Glc in the labeled perfusion aCSF was $10\,\mathrm{mM}$, it is possible that the actual concentration in the NMR tube is lower because of incomplete washout of the non-labeled perfusion aCSF during the transfer to the labeled aCSF; and (2) although H²HO is at the same concentration in all water compartments (perfusion medium, extracellular space, and intracellular space), 2H_2 -Glc may not occupy these compartments equally; for example, the intracellular

compartment is likely to have a lower concentration of $^2\mathrm{H}_2$ -Glc because of the quick metabolic conversion by glycolysis. Therefore, the overall $^2\mathrm{H}_2$ -Glc concentration in the perfusion aCSF may be underestimated. In the same way, $^2\mathrm{H}_2$ -Lac is likely present predominantly in the intracellular compartment (see section below). Hence, its concentration value does not reflect the concentration in this compartment.

In addition, we have not considered the effect of motion on the SNR of these signals. Moving spins contribute less to the SNR than non-moving spins. However, we did not quantify this effect; because of the T_1 difference, it likely differs between 2H_2 -Glc and H^2HO , which both predominantly originate from the medium, that is, from moving spins. To omit the influence of motion on the measurement of the 2H_2 -Lac signal in the medium, we carried out this measurement under the same flow conditions (after removing the brain slices that produced this 2H_2 -Lac) from the NMR tube (see Results). However, for the measurements in brain slices, as the 2H_2 -Lac signal originates mainly from within the cells (see below), that is, from non-moving spins, its concentration in the NMR tube is likely overestimated compared to H^2HO .

5.2 | The Compartment of the ²H₂-Lac Signal

We consider ²H₂-Lac to be predominantly intracellular based on the finding that after 5h in the presence of ${}^2\mathrm{H}_2$ -Glc, the ${}^2\mathrm{H}_2$ -Lac signal in the medium was only 2.2% of the level of ²H₂-Lac in the NMR tube containing the brain slices. This result was obtained in the same NMR tube containing the same perfusion lines and temperature sensor, and with the same perfusion rate as the perfusion of the slices, after removal of the brain slices from the NMR tube. This was done to avoid flow-related T₁ effects or homogeneity differences that may influence the signal intensities of H2HO and 2H2-Lac. The entire volume of the perfusion medium (in the bottle, in the perfusion tubes, and the NMR tube) at any given moment was 70 mL, and the volume of the sensitive area of the probe was 1.375 mL. Therefore, even if all the 2H2-Lac detected in the perfusion medium were concentrated in the sensitive volume of the probe (and the perfusion would be halted), it would make only a 1.12-fold higher signal of the ²H₂-Lac signal during continuous flow (2.2%*70/1.375), which is an insignificant increase. As this is not the case during constant flow, and as the 2H2-Lac signal increased more than fivefold during the perfusion arrest, it suggests that the ²H₂-Lac signal of perfused brain slices predominantly arises from within the cells in the brain slices, which were located within the NMR tube in the detection region of the probe throughout experiments. In agreement, our previous studies with the same perfused rat brain slices system and hyperpolarized ¹³C-labeled pyruvate showed that labeled lactate was constantly produced in the slices during both continuous perfusion and perfusion arrest [9, 10]. Nevertheless, we cannot exclude that during perfusion arrest (during the ischemic condition), the ²H₂-Lac that accumulates may be partly washed out to the medium inside the NMR tube, because there is no washout from the NMR tube. However, if this is correct, it will likely also occur in vivo, as the washout and wash-in to the ischemic region are lower. For example, cerebral collateral circulation in humans provides perfusion to the hypoperfused penumbra with a delay of less than 10 s

and a reduced relative cerebral blood flow (rCBF \leq 30%) [23]. This reduction of flow, while detrimental to brain function, is not expected to limit a potential delivery of $^2\mathrm{H}_2$ -Glc to the region of interest, although it may restrict the washout of the potentially released $^2\mathrm{H}_2$ -Lac.

In future studies, we intend to investigate the effect of perfusion rate on glucose metabolism in brain slices. We note that oxygen–glucose deprivation, which is a consequence of stroke, has been investigated in the same perfused brain slices setup [24]. However, it appears that a reduction in flow (both wash-in and washout) will represent AIS better. At any rate, the current study serves as proof of concept for the feasibility of this approach, and we consider it a starting point for a comprehensive study on the effects of flow on glucose metabolism in the brain.

5.3 | High or Low Glc?

The Glc concentration here reached 4 mM during ischemia, which is not considered a low concentration that would be experienced during stroke. However, this was reduced from a baseline of ~10 mM. High Glc and oxygen conditions are intentionally provided in brain slice preparations. This is because Glc and oxygen reach the depth of the slices by diffusion, which is influenced by the concentration gradient (more information on this aspect is provided in the Materials and Methods in the subsection "Oxygen Concentration in the aCSF Solutions"). To reach physiological levels of Glc and oxygen in the middle of the slice and sustain viability throughout the slice, Glc and oxygen must be provided at higher than physiological concentrations. This differs from the in vivo scenario because nutrients and oxygen are not delivered via the vasculature. Therefore, as the Glc concentration decreases in the buffer, it decreases much more slices' cores. Preserving the viability of brain slices in the same system, without any insults or perturbations, with 5-mM Glc in the aCSF is not beneficial. The ATP in brain slices perfused with aCSF containing only 5-mM Glc decreases rapidly (unpublished results).

5.4 | The Rodent Brain as a Model of the Human Brain?

Although the fundamental biochemical machinery that metabolizes nutrients is relatively conserved among mammalian species brains, the human brain metabolism differs from the rodent brain metabolism in factors that may affect its susceptibility to ischemic stroke. This has been shown by comparing brain metabolism in brain slices from mice and humans by Westi et al. in 2022 [25]. In addition, in recent years, it has become evident that the results of stroke studies in rodents are not fully translatable to humans, and the use of animals with large gyrencephalic human-like brains as opposed to small lissencephalic brains has been proposed [26, 27]. Several recent studies have developed stroke models in the common pig and in miniature pigs [26, 27]. These considerations may limit the translation of results from the rodent brain to the human brain. Nevertheless, we note that the porcine models of stroke are technically complex and costly. In the absence of a better option for in vivo and ex vivo studies, to the best of our knowledge, most of the studies on ischemic stroke have been carried out in rodent animal models.

5.5 | Translation—Local Versus Global Phenomenon

AIS in human adults is typically a localized brain phenomenon with an ischemic core and a threatened penumbra, and otherwise mostly normally functioning brain. In the current model, we sought to model the normally functioning brain versus the threatened penumbra. We did not seek to model the ischemic core, as that would be a tissue without metabolism. The normal functioning brain is modeled by the brain slices before an ischemic insult, and the threatened penumbra is modeled using the same slices during an ischemic insult. While the approach may have cons compared to studies of in vivo imaging, which may show simultaneously all three states (normal functioning brain, ischemic core, and threatened penumbra), it has the advantage of researching a homogeneous state without overlap with other states in the image plane.

6 | Hope for the Future

There are currently two treatment options for AIS: fibrinolytic agents (such as alteplase or tenecteplase) and mechanical thrombectomy [28]. Hypothermia is often used to reduce neuronal injury, and additional pharmaceutical interventions are a desperate medical need [29]. Although numerous agents showed utility preclinically, most have failed in clinical trials. However, the search for neuroprotective agents continues, with increasing evidence that the irreversible damage to ischemic brain tissue is mainly due to factors after the lack of blood flow and oxygen (i.e., during reperfusion). Of the promising neuroprotective agents that were studied recently, preclinically and clinically, we note edaravone dexborneol [30], RNS60 [31, 32], and tatCN190 [33], which, by distinctly different mechanisms, can reduce the infarct size and improve the recovery from AIS. Our findings suggest that the dynamics of glucose metabolism under normal flow, flow arrest, and reperfusion can be investigated in rat brain slices using ²H₂-Glc and ²H-NMR with high fidelity. In addition, our findings further support the ability of the current model to contribute to brain ischemia studies. We hope that this model (perfused rat brain slices, perfusion arrest, and reperfusion) and the current approach (2H-NMR of 2H₂-Glc) will provide a useful system for the development of new therapies for stroke.

Author Contributions

Rachel Katz-Brull, J. Moshe Gomori, and David Shaul designed the study. Rachel Katz-Brull obtained funding for this study and supervised all the work. David Shaul and Sara Abendanan performed the experiments. Sara Abendanan analyzed all the ²H-NMR results. David Shaul analyzed the ³¹P-NMR results. Sara Abendanan produced all the figures and tables in the manuscript and wrote the first draft together with Rachel Katz-Brull. All authors contributed to the writing of the manuscript and approved the final version.

Acknowledgments

We thank Dr. Ayelet Gamliel and Ms. Shira Rachlin for their technical assistance in the studies. This study has received funding from the European Commission (Grant/Award Number 101185775—DDG-MRI), the Israel Ministry of Science, Innovation and Technology

(Grant/Award Number 1001704106/0006244), and the Israel Innovation Authority (Grant/Award Number 84405).

Data Availability Statement

Data are available in the Supporting Information section of this article.

References

- 1. WHO, "The Top 10 Causes of Death," (2024), Retrieved: July 28, 2024, https://www.who.int/news-room/fact-sheets/detail/the-top-10-cause s-of-death.
- 2. T. B. Rodrigues and J. V. Bouzier-Sore, "A K. 13C NMR Spectroscopy Applications to Brain Energy Metabolism," *Frontiers in Neuroenergetics* 5 (2013): 9, https://doi.org/10.3389/fnene.2013.00009.
- 3. G. J. Siegel, B. W. Agranoff, and R. W. Albers, *Basic Neurochemistry: Molecular, Cellular and Medical Aspects*, 6th ed. (*Lippincott-Raven*, 1999).
- 4. O. E. Owen, A. P. Morgan, H. G. Kemp, J. M. Sullivan, M. G. Herrera, and G. F. Cahill, "Brain Metabolism During Fasting," *Journal of Clinical Investigation* 46, no. 10 (1967): 1589–1595, https://doi.org/10.1172/jci105650.
- 5. F. A. X. Schanne, R. K. Gupta, and P. K. Stanton, "P-31-NMR Study of Transient Ischemia in Rat Hippocampal Slices In Vitro," *Biochimica et Biophysica Acta* 1158, no. 3 (1993): 257–263, https://doi.org/10.1016/0304-4165(93)90023-2.
- 6. M. T. Espanol, L. Litt, L. H. Chang, T. L. James, P. R. Weinstein, and P. H. Chan, "Adult Rat Brain-Slice Preparation for Nuclear Magnetic Resonance Spectroscopy Studies of Hypoxia," *Anesthesiology* 84, no. 1 (1996): 201–210, https://doi.org/10.1097/00000542-199601000-00022.
- 7. S. Komatsumoto, S. Nioka, J. H. Greenberg, et al., "Cerebral Energy-Metabolism Measured In Vivo by p-31-NMR in Middle Cerebral-Artery Occlusion in the Cat Relation to Severity of Stroke," *Journal of Cerebral Blood Flow and Metabolism* 7, no. 5 (1987): 557–562, https://doi.org/10.1038/jcbfm.1987.105.
- 8. S. R. Levine, K. M. A. Welch, J. A. Helpern, et al., "Prolonged Deterioration of Ischemic Brain Energy-Metabolism and Acidosis Associated With Hyperglycemia Human Cerebral Infarction Studied by Serial p-31 NMR-Spectroscopy," *Annals of Neurology* 23, no. 4 (1988): 416–418, https://doi.org/10.1002/ana.410230423.
- 9. G. Sapir, D. Shaul, N. Lev-Cohain, J. Sosna, J. M. Gomori, and R. Katz-Brull, "LDH and PDH Activities in the Ischemic Brain and the Effect of Reperfusion—An Ex Vivo MR Study in Rat Brain Slices Using Hyperpolarized [1-13C]pyruvate," *Metabolites* 11, no. 4 (2021): 210, https://doi.org/10.3390/metabol1040210.
- 10. D. Shaul, B. Grieb, G. Sapir, et al., "The Metabolic Representation of Ischemia in Rat Brain Slices: A Hyperpolarized ¹³C Magnetic Resonance Study," *NMR in Biomedicine* 34 (2021): e4509, https://doi.org/10.1002/nbm.4509.
- 11. H. M. De Feyter, K. L. Behar, Z. A. Corbin, et al., "Deuterium Metabolic Imaging (DMI) for MRI-Based 3D Mapping of Metabolism In Vivo," *Science Advances* 4, no. 8 (2018): eaat7314, https://doi.org/10.1126/sciadv.aat7314.
- 12. J. D. Kaggie, A. S. Khan, T. Matys, et al., "Deuterium Metabolic Imaging and Hyperpolarized (13)C-MRI of the Normal Human Brain at Clinical Field Strength Reveals Differential Cerebral Metabolism," *Neuroimage* 257 (2022): 119284, https://doi.org/10.1016/j.neuroimage.2022. 119284.
- 13. A. Taha, J. Bobi, R. Dammers, et al., "Comparison of Large Animal Models for Acute Ischemic Stroke: Which Model to Use?," *Stroke* 53, no. 4 (2022): 1411–1422, https://doi.org/10.1161/strokeaha.121.036050.
- 14. J. T. Ting, T. L. Daigle, Q. Chen, and G. Feng, "Acute Brain Slice Methods for Adult and Aging Animals: Application of Targeted Patch

- Clamp Analysis and Optogenetics," in *Patch-Clamp Methods and Protocols* (Springer, 2014): 221–242.
- 15. R. Katz-Brull, R. Margalit, P. Bendel, and H. Degani, "Choline Metabolism in Breast Cancer; (2)H-, (13)C- and (31)P-NMR Studies of Cells and Tumors," *Magnetic Resonance Materials in Physics, Biology and Medicine (MAGMA)* 6, no. 1 (1998): 44–52, https://doi.org/10.1016/s1352-8661(98)00009-x.
- 16. O. Benyoseph, P. B. Kingsley, and B. D. Ross, "Metabolic Loss of Deuterium From Isotopically Labeled Glucose," *Magnetic Resonance in Medicine* 32, no. 3 (1994): 405–409, https://doi.org/10.1002/mrm.19103 20317.
- 17. R. A. de Graaf, M. A. Thomas, K. L. Behar, and H. M. De Feyter, "Characterization of Kinetic Isotope Effects and Label Loss in Deuterium-Based Isotopic Labeling Studies," *ACS Chemical Neuroscience* 12, no. 1 (2021): 234–243, https://doi.org/10.1021/acschemneuro.0c00711.
- 18. B. Grieb, S. Uppala, G. Sapir, D. Shaul, J. M. Gomori, and R. Katz-Brul, "Curbing Action Potential Generation or ATP-Synthase Leads to a Decrease in In-Cell Pyruvate Dehydrogenase Activity in Rat Cerebrum Slices," *Scientific Reports* 11 (2021): 10211, https://doi.org/10.1038/s4159 8-021-89534-4.
- 19. M. El Hage, B. Ferrier, G. Baverel, and G. Martin, "Rat Brain Slices Oxidize Glucose at High Rates: A ¹³C NMR Study," *Neurochemistry International* 59, no. 8 (2011): 1145–1154, https://doi.org/10.1016/j.neuint. 2011.10.009.
- 20. F. A. Welsh, J. H. Greenberg, S. C. Jones, M. D. Ginsberg, and M. Reivich, "Correlation between glucose utilization and metabolite levels during focal ischemia in cat brain," *Stroke* 11, no. 1 (1980): 79–84, https://doi.org/10.1161/01.str.11.1.79.
- 21. D. J. Combs, R. J. Dempsey, M. Maley, D. Donaldson, and C. Smith, "Relationship between plasma glucose, brain lactate, and intracellular pH during cerebral ischemia in gerbils," *Stroke* 21, no. 6 (1990): 936–942, https://doi.org/10.1161/01.str.21.6.936.
- 22. P. Bagga, K. L. Behar, G. F. Mason, H. M. De Feyter, D. L. Rothman, and A. B. Patel, "Characterization of cerebral glutamine uptake from blood in the mouse brain: implications for metabolic modeling of 13C NMR data," *Journal of Cerebral Blood Flow and Metabolism* 34, no. 10 (2014): 1666–1672, https://doi.org/10.1038/jcbfm.2014.129.
- 23. Y. Yu, Q. Han, X. Ding, et al., "Defining Core and Penumbra in Ischemic Stroke: A Voxel- and Volume-Based Analysis of Whole Brain CT Perfusion," *Scientific Reports* 6 (2016): 20932, https://doi.org/10.1038/srep20932.
- 24. A. Molska, D. K. Hill, T. Andreassen, and M. Wideroe, "Perfusion system for studying dynamic metabolomics in rat brain slices exposed to oxygen–glucose deprivation using proton and phosphorus nuclear magnetic resonance," *NMR in Biomedicine* 36 (2022): e4703, https://doi.org/10.1002/nbm.4703.
- 25. E. W. Westi, E. Jakobsen, C. M. Voss, et al., "Divergent cellular energetics, glutamate metabolism, and mitochondrial function between human and mouse cerebral cortex," *Molecular Neurobiology* 59, no. 12 (2022): 7495–7512, https://doi.org/10.1007/s12035-022-03053-5.
- 26. F. Arikan, T. Martinez-Valverde, A. Sanchez-Guerrero, et al., "Malignant infarction of the middle cerebral artery in a porcine model. A pilot study," *PLoS ONE* 12, no. 2 (2017): e0172637, https://doi.org/10.1371/journal.pone.0172637.
- 27. A. J. Sorby-Adams, R. Vink, and R. J. Turner, "Large animal models of stroke and traumatic brain injury as translational tools," *American Journal of Physiology. Regulatory, Integrative and Comparative Physiology* 315 (2018): R165–R190.
- 28. C. Zerna, G. Thomalla, B. C. V. Campbell, J. H. Rha, and M. D. Hill, "Current practice and future directions in the diagnosis and acute treatment of ischaemic stroke," *Lancet* 392, no. 10154 (2018): 1247–1256, https://doi.org/10.1016/s0140-6736(18)31874-9.

- 29. M. Fisher and S. I. Savitz, "Pharmacological brain cytoprotection in acute ischaemic stroke—renewed hope in the reperfusion era. Nature Reviews," *Neurology* 18, no. 4 (2022): 193–202, https://doi.org/10.1038/s41582-021-00605-6.
- 30. R. Y. Hu, J. Liang, L. Ding, et al., "Edaravone dexborneol provides neuroprotective benefits by suppressing NLRP3 inflammasome-induced microglial pyroptosis in experimental ischemic stroke," *International Immunopharmacology* 113, no. 109 (2022): 315, https://doi.org/10.1016/j.intimp.2022.109315.
- 31. G. P. Baena-Caldas, J. Li, L. Pedraza, et al., "Neuroprotective effect of the RNS60 in a mouse model of transient focal cerebral ischemia," *PLoS ONE* 19, no. 1 (2024): e0295504, https://doi.org/10.1371/journal.pone.0295504.
- 32. L. Murray "Stroke patients discharged from hospital sooner when administered Revalesio's RNS60; New statistically significant finding from Revalesio's phase 2 clinical trial," retrieved April 9, 2025, https://www.prnewswire.com/news-releases/stroke-patients-discharged-from-hospital-sooner-when-administered-revalesios-rns60-newstatistically-significant-finding-from-revalesios-phase-2-clinical-trial -302423981.html.
- 33. N. L. Rumian, C. N. Brown, T. B. Hendry-Hofer, et al., "Short-term CaMKII inhibition with tatCN190 does not erase pre-formed memory in mice and is neuroprotective in pigs," *Journal of Biological Chemistry* 299, no. 5 (2023): 104693, https://doi.org/10.1016/j.jbc.2023.104693.

Supporting Information

Additional supporting information can be found online in the Supporting Information section. **Table S1:** A summary of individual data used for statistical analysis is in the Results section. **Figure S1:** ^{31}P NMR spectra of the brain slices during the three ischemia experiments. Information about the timing of acquiring the individual spectra is provided in the table below. Signal assignment: 1, phosphomonoesters; 2, inorganic-phosphate; 3, phosphocreatine; 4, γ -adenosine triphosphate $(\gamma$ -ATP); 5, α -ATP; and 6, β -ATP. Phosphocreatine served as a reference for chemical shift at $-2.5\,\mathrm{ppm}$. **Figure S2:** A part of the time course of the experiment with three ischemic conditions, showing the time course of the $^2\mathrm{H}_x$ -Glx signal in this experiment. The entire course of this experiment is shown in Figure 3C. X=0 here is at the start of the reperfusion after the first ischemic condition, where the $^2\mathrm{H}_x$ -Glx signal was first observed. Breaks in $^2\mathrm{H}\text{-NMR}$ acquisitions are taken to record $^{31}\mathrm{P}$ spectra.